the plant journal

SEB Society for Experimental Biology

The Plant Journal (2017) **89,** 381–393 doi: 10.1111/tpj.13391

Dysfunction of Arabidopsis MACPF domain protein activates programmed cell death via tryptophan metabolism in MAMP-triggered immunity

Satoshi Fukunaga[1], Miho Sogame[1], Masaki Hata[1], Suthitar Singkaravanit-Ogawa[1], Mariola Piślewska-Bednarek[2], Mariko Onozawa-Komori[1], Takumi Nishiuchi[3], Kei Hiruma[4], Hiromasa Saitoh[5], Ryohei Terauchi[5], Saeko Kitakura[1], Yoshihiro Inoue[1], Paweł Bednarek[2], Paul Schulze-Lefert[6] and Yoshitaka Takano[1,*]

[1]*Graduate School of Agriculture, Kyoto University, Kyoto, Japan,*
[2]*Institute of Bioorganic Chemistry, Polish Academy of Sciences, Poznan, Poland,*
[3]*Advanced Science Research Center, Kanazawa University, Kanazawa, Japan,*
[4]*Graduate School of Biological Sciences, Nara Institute of Science and Technology, Ikoma, Japan,*
[5]*Iwate Biotechnology Research Center, Iwate, Japan, and*
[6]*Department of Plant-Microbe Interactions, Max Planck Institute for Plant Breeding Research, Cologne, Germany*

Received 24 February 2016; revised 30 September 2016; accepted 3 October 2016; published online 7 January 2017.
*For correspondence (e-mail ytakano@kais.kyoto-u.ac.jp).

SUMMARY

Plant immune responses triggered upon recognition of microbe-associated molecular patterns (MAMPs) typically restrict pathogen growth without a host cell death response. We isolated two Arabidopsis mutants, derived from accession Col-0, that activated cell death upon inoculation with nonadapted fungal pathogens. Notably, the mutants triggered cell death also when treated with bacterial MAMPs such as flg22. Positional cloning identified *NSL1* (*Necrotic Spotted Lesion 1*) as a responsible gene for the phenotype of the two mutants, whereas *nsl1* mutations of the accession No-0 resulted in necrotic lesion formation without pathogen inoculation. *NSL1* encodes a protein of unknown function containing a putative membrane-attack complex/perforin (MACPF) domain. The application of flg22 increased salicylic acid (SA) accumulation in the *nsl1* plants derived from Col-0, while depletion of isochorismate synthase 1 repressed flg22-inducible lesion formation, indicating that elevated SA is needed for the cell death response. *nsl1* plants of Col-0 responded to flg22 treatment with an RBOHD-dependent oxidative burst, but this response was dispensable for the *nsl1*-dependent cell death. Surprisingly, loss-of-function mutations in *PEN2,* involved in the metabolism of tryptophan (Trp)-derived indole glucosinolates, suppressed the flg22-induced and *nsl1*-dependent cell death. Moreover, the increased accumulation of SA in the *nsl1* plants was abrogated by blocking Trp-derived secondary metabolite biosynthesis, whereas the *nsl1*-dependent hyperaccumulation of PEN2-dependent compounds was unaffected when the SA biosynthesis pathway was blocked. Collectively, these findings suggest that MAMP-triggered immunity activates a genetically programmed cell death in the absence of the functional MACPF domain protein NSL1 via Trp-derived secondary metabolite-mediated activation of the SA pathway.

Keywords: MACPF domain, MAMPs, cell death, Tryptophan-derived metabolism, salicylic acid signaling, secondary metabolites, *Colletotrichum orbiculare*.

INTRODUCTION

Effective innate immunity in higher plants often depends on the activation of two interconnected immune responses that limit or terminate pathogen growth. Activation of immune responses mediated by the recognition of microbe-associated molecular patterns (MAMPs) on the plant cell surface is referred to as MAMP-triggered immunity (MTI) and limits pathogen proliferation. Several membrane-resident receptor-like kinases, including FLS2, EFR, and CERK1, have been characterized as MAMP receptors for the extracellular detection of evolutionarily broadly conserved microbial epitopes present in bacterial flagellin, the translation elongation factor EF-Tu or the fungal cell wall component chitin, respectively (Boller and Felix, 2009; Schwessinger and Ronald, 2012).

MTI is generally sufficient to terminate infection attempts of nonadapted pathogens. However, host-adapted pathogens can suppress MTI by the delivery of a repertoire of virulence factors, called effectors, which act either extracellularly or inside host cells. As counter-defense mechanism against this effector-mediated infection strategy, intracellular nucleotide-binding domain and leucine-rich repeat containing receptors (NLRs) re-activate immune responses upon the detection of often strain-specific pathogen effectors. NLRs detect the presence of cognate effectors inside host cells either directly or indirectly through effector-mediated modifications of host targets (Dodds and Rathjen, 2010; Maekawa *et al.*, 2011). The detection of pathogen-derived effectors by NLR immune receptors initiates a rapid, and local immune response, known as effector-triggered immunity (ETI) (Tsuda and Katagiri, 2010). In many cases ETI is associated with a form of programmed cell death (PCD), which is called the hypersensitive response (Heath, 2000a). By contrast, MTI-mediated defense responses are transient and usually not associated with a PCD. Interestingly, although the output of MTI is normally different from that of ETI, both branches overlap significantly with each other in terms of host gene expression and defensive traits (Navarro *et al.*, 2004; Tsuda and Katagiri, 2010).

We aim to identify molecular components and pathways underlying durable resistance of *Arabidopsis thaliana* toward nonadapted pathogens, called nonhost resistance (Heath, 2000b; Schulze-Lefert and Panstruga, 2011). We are particularly interested in *Colletotrichum* fungal species that exhibit a hemibiotrophic infection strategy (Perfect *et al.*, 1999; Shimada *et al.*, 2006). In hemibiotrophic interactions the fungus initially invades and retrieves nutrients from living host cells and switches to a necrotrophic colonization mode at later infection stages by killing host cells for nutrient retrieval. To identify factors involved in nonhost resistance of Arabidopsis against *C. orbiculare* that infects *Cucurbitaceae* plants in nature (Gan *et al.*, 2013; Kubo and Takano, 2013), we screened for Arabidopsis mutants that develop leaf lesions upon *C. orbiculare* spore inoculation. The mutant survey identified two allelic mutants in accession Col-0 that we named *lic1* (*lesion induced by Colletotrichum 1*). Further analysis revealed that mutations in *At1g28380* were responsible for the *lic1* phenotype. Two independent mutations in the same gene have been previously reported to be responsible for the *nsl1* (*necrotic spotted lesion 1*) phenotype in the Arabidopsis accession No-0 (Noutoshi *et al.*, 2006). Both *nsl1* mutants (*nsl1-1* and *nsl1-2*) of the accession No-0 show severe growth retardation and spontaneous necrotic leaf lesions, which is not the case for both *lic1-1* and *lic1-2* mutants of the accession Col-0, renamed *nsl1-3* and *nsl1-4,* respectively.

NSL1 encodes a protein containing a putative membrane-attack complex/perforin (MACPF) domain. It is known that several mammalian MACPF domain proteins play important roles in immunity by forming pores in the cell membranes of pathogenic parasites, such as Gram-negative bacteria, or in the membranes of virus-infected host cells, thereby causing these cells to burst (Rosado *et al.*, 2008; McCormack *et al.*, 2013). Structural determination of the MACPF domain revealed that MACPF is structurally homologous to the pore-forming toxins of Gram-positive bacteria, called cholesterol-dependent cytolysins (Rosado *et al.*, 2007). However, there is little information about the molecular function of MACPF domain proteins, including NSL1, in higher plants.

Here we generated stable transgenic Arabidopsis lines expressing functional green fluorescent protein (GFP)–NSL1 fusion protein and revealed that NSL1 localizes to the plasma membrane of Arabidopsis leaf cells. We found that the application of peptide bacterial MAMPs such as flg22 (a 22-amino acid peptide corresponding to a conserved epitope of bacterial flagellin) or elf18 (elongation factor Tu N-acetylated peptide, comprising the first 18 amino acids of the N-terminus) also induced leaf lesions in the *nsl1-3* and *nsl1-4* mutants (Col-0 background). These findings indicated that, in wild-type Arabidopsis, MAMP-induced cell death is repressed by the plasma membrane-associated MACPF protein. We then dissected the genetic circuitry underlying the MAMP-induced cell death response in the *nsl1* mutants and found that loss-of-function mutations in penetration 2 (*PEN2*) largely abolish the MAMP-induced and *nsl1*-dependent cell death. *PEN2* is known to be essential for the pathogen-inducible metabolism of Trp-derived indole glucosinolates (IGs) and nonhost resistance of Arabidopsis against multiple nonadapted fungal pathogens (Lipka *et al.*, 2005; Hiruma *et al.*, 2010). Our findings reveal an unexpected link between pathogen-induced antimicrobial metabolism and MAMP-induced cell death. Further analyses revealed that antimicrobial metabolites activate salicylic acid (SA) signaling to trigger cell death during MTI in the absence of the functional MACPF domain protein.

RESULTS

Mutations in Arabidopsis *NSL1* lead to the development of necrotic leaf lesions upon *C. orbiculare* inoculation

To identify genetic components contributing to nonhost resistance in *A. thaliana* we screened an Arabidopsis mutant population for plants that formed leaf lesions upon inoculation with nonadapted *C. orbiculare* (*Co*), which in nature colonizes cucumber (Kubo and Takano, 2013). Among about 6000 ethyl methanesulfonate mutagenized M_2 Col-0 plants we identified two independent Arabidopsis mutants, designated L1 and L2, that formed necrotic leaf lesions accompanied by whole leaf yellowing upon inoculation with *Co* spores (Figure 1(a)). F_1 progeny obtained

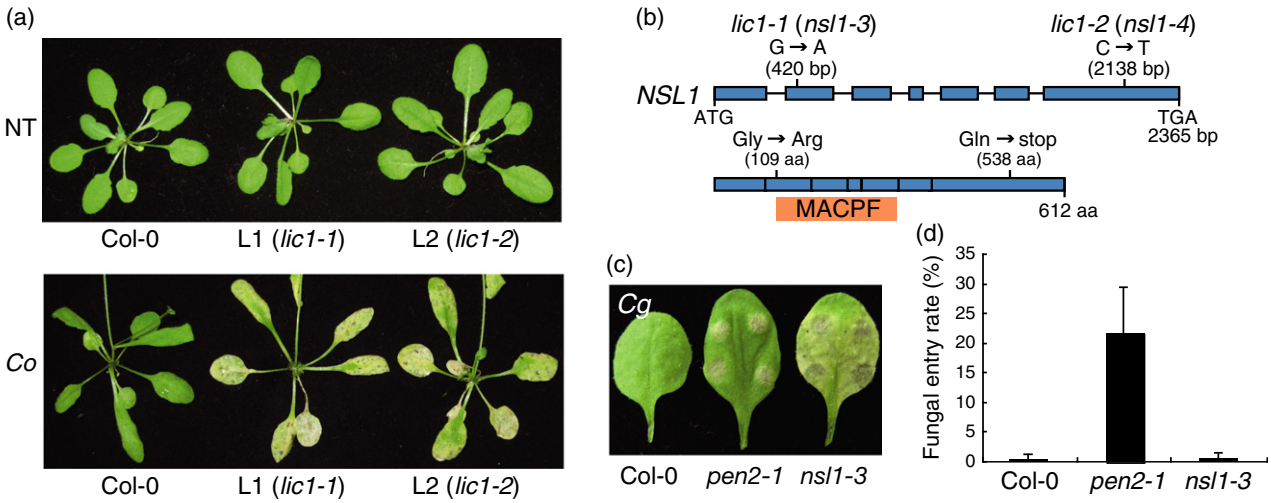

Figure 1. Identification of Arabidopsis *nsl1* mutants in Col-0 background.
(a) The lesion phenotype of the *lic1* mutants of Arabidopsis Col-0 under inoculation with nonadapted pathogen *C. orbiculare* (*Co*). The two mutants L1 and L2 (*lic1-1* and *lic1-2,* respectively) showed the WT phenotype without pathogen treatment (NT) but developed severe necrotic lesions after inoculation with *Co*. The WT Col-0 plants did not form any lesions. A conidial suspension of *Co* was spray-inoculated on the tested lines, and the inoculated plants were incubated for 6 days.
(b) Mutations in *NSL1* are responsible for the *lic1* phenotype. Exons and introns are indicated by blue boxes and horizontal lines, respectively. The position of the MACPF domain is indicated by the orange box. *lic1-1* and *lic1-2* was renamed as *nsl1-3* and *nsl1-4,* respectively.
(c) The lesion phenotype of the *nsl1-3* mutant under inoculation with the nonadapted pathogen *C. gloeosporioides* (*Cg*). A conidial suspension of *Cg* was drop-inoculated on the tested lines in the presence of Glc (Hiruma *et al.*, 2010), and the inoculated plants were incubated for 4 days.
(d) *Cg* failed to invade the *nsl-3* mutant. *Cg* was inoculated on the cotyledons of the test plants, and the inoculated plants were incubated for 14 h. Invasion of germinating conidia was investigated. At least 100 conidia were observed in each experiment. The means and standard deviations (SDs) were calculated from three independent experiments.

from crosses between L1 and L2 mutants exhibited the same necrotic leaf lesion phenotype upon *Co* challenge, suggesting that both mutants might carry allelic gene defects, designated *lic1* (*lesion induced by Colletotrichum 1*). Positional cloning using F_2 populations obtained from crosses between L2 (*lic1-2*) and the accession L*er* mapped the *lic1* allele between SGCSNP 9883 (9880523 bp) and SGCSNP9897 (10007758 bp) on chromosome 1.

DNA polymorphisms between Col-0 and the two *lic1* mutants of this region were investigated using the TILLING (targeting induced local lesions in genomes) method (McCallum *et al.*, 2000). The L1 (*lic1-1*) and L2 (*lic1-2*) polymorphisms were found in the same gene *At1g28380* previously named *Necrotic Spotted Lesions1* (*NSL1*) (Noutoshi *et al.*, 2006) (Figures 1(b) and S1). Sequencing of the entire region of *NSL1* revealed that L1 has a mutation at nucleotide position 420 that changes Gly to Arg at amino acid residue 109, whereas L2 has a mutation at nucleotide position 2,138 that changes Gln to a stop codon at amino acid residue 538. We concluded that these *NSL1* mutations are responsible for the *lic1* phenotype. Previously, two independent transposon insertions into *NSL1* (*nsl1-1* and *nsl1-2*) in the Arabidopsis accession No-0 resulted in dwarfism and leaf lesions in the absence of microbial pathogens (Noutoshi *et al.*, 2006), which is distinct from the phenotype of L1 (*lic1-1*) and L2 (*lic1-2*) exhibiting no lesion phenotype in the absence of pathogens (Figure 1(a)). We hereafter call *lic1-1* and *lic1-2* as *nsl1-3* and *nsl1-4,* respectively. *NSL1* encodes a protein of unknown function that contains a putative MACPF domain (Rosado *et al.*, 2008; McCormack *et al.*, 2013). The *nsl1-3* mutation affects in the *NSL1* gene product an amino acid adjacent to the N-terminal end of a deduced MACPF domain whereas the *nsl1-4* mutation predicts a truncation at a distance from this domain close to the NSL1 C-terminus (Figures 1(b) and S1).

Colletotrichum gloeosporioides (*Cg;* strain S9205) infects mulberry but cannot infect Arabidopsis because *Cg* entry attempts of fungal germlings into leaf epidermal cells are terminated by pathogen-inducible extracellular defense responses (Shimada *et al.*, 2006; Hiruma *et al.*, 2010). We previously reported that nonadapted *Cg* grows invasively in Arabidopsis *pen2* plants that are defective in pre-invasive resistance responses, and that subsequent invasive growth is accompanied by leaf lesion formation (Lipka *et al.*, 2005; Hiruma *et al.*, 2010). We found that *Cg* also induced leaf lesions on the *nsl1-3* mutant. In addition, a leaf yellowing was seen outside the *Cg*-inoculated area of *nsl1-3* plants, whereas any macroscopically detectable infection symptoms were confined to the droplet inoculated leaf area in the *pen2* mutant (Figure 1(c)).

We determined fungal entry rates of *Cg* germlings into *nsl1-3* leaf epidermal cells and found these were similar to entry rates on wild-type (WT) plants (close to 0%), whereas

fungal entry on *pen2* plants was about 20% (Figure 1(d)). These results indicate that nonhost resistance of the *nsl1* plants in entry control against *Cg* is fully retained although *Cg* inoculation induced necrotic lesion development. This uncoupling of lesion development from *Cg* invasion pointed at the possibility that cell death was improperly activated in the *nsl1* mutants coincident with pre-invasive pathogenesis of nonadapted *Co* and *Cg*. As mentioned, the *nsl1-1* and *nsl1-2* mutants of the accession No-0 developed dwarfism and leaf lesions in the absence of microbial pathogens (Noutoshi *et al*., 2006). Although the *nsl1-3* and *-4* mutants of Col-0 were neither dwarfed nor developed leaf lesions in pathogen-free environments, our findings and those reported earlier suggest that *NSL1* (*At1g28380*) has a role in cell death repression in the absence of pathogens as well as during pathogen-triggered plant defense.

MAMP-induced cell death in *the nsl1* mutants

The finding that *nsl1*-dependent leaf lesion formation in Col-0 is uncoupled from pathogen invasion raised the possibility that extracellular pathogen recognition is sufficient for the activation of *nsl1*-dependent cell death. The presence of a number of well characterized MAMPs, including the bacterium-derived flg22 and elf18 epitopes, is recognized by corresponding membrane-resident pattern recognition receptors (PRRs) on the host cell surface, which initiates MTI (Boller and Felix, 2009; Schwessinger and Ronald, 2012). We investigated whether MAMP treatment can induce the lesion phenotype in the *nsl1-3* and *nsl1-4* mutants by administering droplets containing a bacterium-derived MAMP on the leaf surface of the tested plant lines. As a result, treatment with flg22 at 10 μM resulted in clear necrotic lesions in mature leaves and cotyledons on both *nsl1* mutant lines but not WT plants (Figure 2(a)). Lesions also developed on cotyledons of the *nsl1* mutant seedlings upon treatment with the same MAMP (Figure 2(b)). Infiltration of flg22 at 1 μM also induced lesion development in *nsl1-3* but not in WT (Figure S2(b)). Droplet application of 10 μM elf18 triggered lesion formation in the mutants but not in WT plants (Figure 2(c)), and the activity of elf18 to induce lesions was higher than that of flg22 (Figure S2(a)). These findings show that the leaf surface treatment with both tested peptide MAMPs derived from bacteria is sufficient to induce leaf lesions in the *nsl1* mutants, indicating a peptide MAMP-triggered cell death response in this mutant background. Next we assessed whether the fungus-derived MAMP chitin is involved in the *Co*-triggered lesion formation in the *nsl1* mutants of Col-0. Arabidopsis CERK1 receptor kinase is known to be critical for chitin recognition in Arabidopsis (Miya *et al*., 2007; Wan *et al*., 2008). Thus, we generated the *nsl1-3 cerk1-2* double mutant and inoculated leaves with *Co* spores. This treatment still induced lesion development in the *nsl1 cerk1* mutant (Figure 2(d)), indicating that CERK1-dependent chitin recognition is not essential for the *Co*-triggered and *nsl1*-dependent leaf cell death. It is possible that *nsl1*-dependent cell death in response to *Co* or *Cg* is triggered via extracellular recognition of unknown MAMP(s) shared between these two *Colletotrichum* species.

NSL1 accumulates at the plasma membrane

To investigate both the expression pattern and subcellular localization of NSL1, we generated *nsl1-3* transgenic lines expressing GFP-fused NSL1 under the control of 1.9 kb 5′ regulatory sequences of *NSL1*. Expression of GFP–NSL1 fully suppressed the *nsl1* lesion phenotype upon both MAMP and pathogen treatments, indicating functionality of the GFP–NSL1 fusion protein (Figures 3(a) and S3(a)). GFP–NSL1 fluorescent signals were undetectable in leaf cells in the absence of MAMP; however, a green fluorescent signal was clearly detectable at the cell periphery upon flg22 application (Figure 3(b)). This suggests that the MAMP treatment confers an enhanced accumulation of NSL1. This conclusion was corroborated in a time-course experiment by western blot analysis using anti-GFP antibody and revealed increased GFP-NSL1 steady-state levels at 24 and 48 hours post treatment (hpt) prior to the manifestation of MAMP-induced cell death in the *nsl1* mutants (Figure 3(d)). The GFP–NSL1 signal at the cell periphery was confined to the plasma membrane when the transgenic lines carrying *GFP–NSL1* were treated with flg22 or *Co* (Figures 3(b) and S3(b)), which is distinct from the GFP fluorescence signal detected in the cytoplasm and nuclei of leaf epidermal cells when *GFP* alone was expressed under the control of 5′ regulatory sequences of *NSL1* (Figure S3 (c)). These findings suggest preferential localization of NSL1 at the plasma membrane, which is further supported by a plasmolysis assay conducted with the *GFP–NSL1* line (Figure 3(c)).

Natural genetic variation in Arabidopsis determines the *nsl1* phenotypic outputs

We found marked phenotypic differences between *nsl1-1* and *nsl1-2* mutants in accession No-0 and *nsl1-3* and *nsl1-4* mutants in accession Col-0 (Figure 4(a)). To clarify whether these differences result from mutant allele-specific differences or accession-dependent variation in genetic backgrounds, we crossed the *nsl1-2* mutant with WT Col-0. Nine of the 38 F_2 progeny plants that were homozygous for the *nsl1-2* allele exhibited the spontaneous leaf lesion phenotype and dwarfism similar to the *nsl1-2* parent. However, the phenotype of other F_2 siblings that were also homozygous for *nsl1-2* was indistinguishable from the WT parent (Figure 4(b)). Furthermore, when the *nsl1-2* F_2 progeny lines displaying WT-like growth were treated with flg22, these plants developed local leaf lesions and were indistinguishable from *nsl1-4* mutants (Figure 4(c)). In reciprocal experiments we crossed the *nsl1-4* mutant with

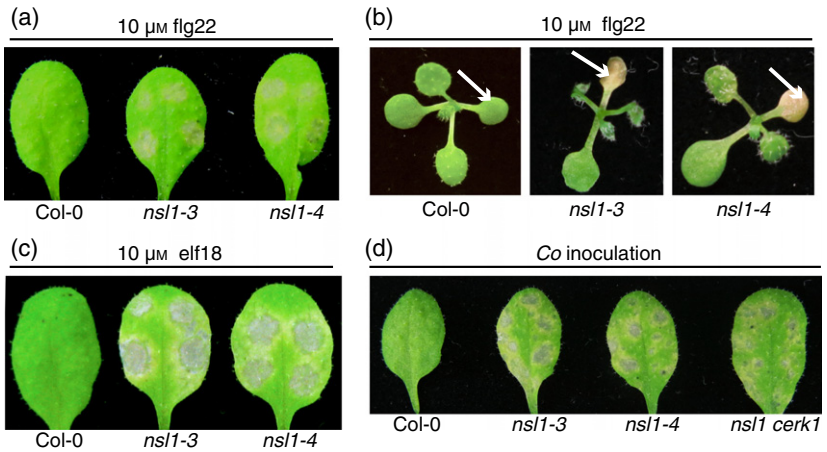

Figure 2. MAMPs trigger programmed cell death in *nsl1* plants.
(a) Bacterial peptide MAMP flg22 induces programmed cell death (PCD) in the *nsl1-3* and *nsl1-4* mutants. The peptide solution was dropped on the leaf surface of the tested Arabidopsis lines, and the treated lines were incubated for 4 days.
(b) flg22 induces PCD in cotyledons of the *nsl1* seedlings. Arrows indicate cotyledons where flg22 solution was spotted.
(c) Bacterial peptide MAMP elf18 induces PCD in the *nsl1* mutants.
(d) CERK1-dependent chitin recognition is not essential for *Co*-induced PCD in *nsl1*. Conidial suspension of *Co* was spray-inoculated on the tested lines, and the inoculated plants were incubated for 6 days.

WT No-0 and selected seven F_2 progeny homozygous for the *nsl1-4* allele and observed that one progeny exhibited stunted plant growth and spontaneous leaf lesions resembling the *nsl1-1* and *nsl1-2* mutants (Figure S4). Together these findings suggest that: (i) the mutations in *At1g28380* (*NSL1*) produce distinct phenotypic outputs in Col-0 and No-0 genetic backgrounds; and that (ii) all four alleles have the potential to cause similar phenotypes, depending on the genetic background of the plants.

flg22-induced PCD in the *nsl1* mutants depends on SA signaling but not on reactive oxygen species (ROS) generation

The dwarf and leaf lesion phenotypes of Arabidopsis *nsl1* plants of the accession No-0 are partially suppressed by a mutation in *SID2* (*EDS16*), which encodes an enzyme necessary for pathogen-induced SA biosynthesis (Wildermuth *et al.*, 2001; Noutoshi *et al.*, 2006). We asked whether the flg22-triggered cell death of the *nsl1* mutants of Col-0 also requires SID2. We generated *nsl1-4 sid2-2* double mutants and found that flg22 did not induce cell death in this line (Figure 5(a)). Similarly, *sid2* abolished pathogen (*Co*)-induced cell death in the *nsl1* background (Figure S5). The *nsl1*- dependent cell death was also reduced by a mutation in *PAD4,* which is involved in SA signaling (Jirage *et al.*, 1999) (Figure S5). These findings indicate that the tested MAMPs trigger PCD in the *nsl1* mutants of Col-0 via the SA pathway.

As cell death in plants is often linked to ROS production we examined hydrogen peroxide accumulation in *nsl1* mutants treated with MAMPs. It is known that MAMP treatment causes rapid ROS production within minutes in the Arabidopsis WT plants. Here we tried to detect hydrogen peroxide (H_2O_2) accumulation by 3′,3′-diaminobenzidine (DAB) staining (Thordal-Christensen *et al.*, 1997) at later time point, i.e., 48 h after MAMP application (before lesions became visible in the *nsl1-3* and *nsl1-4* mutants). Upon flg22 treatment, H_2O_2 accumulation was found to be higher in *nsl1* leaves than in WT plants, indicative of an enhanced ROS accumulation in *nsl1* plants at 48 h after MAMP application (Figure 5(b)). Although the flg22-induced ROS accumulation in the *nsl1 sid2* double mutant at 48 h was similar to that in *nsl1* plants (Figure 5(b)), the flg22-induced lesion formation was strongly diminished in this double mutant (Figure 5(a)). This finding suggests that SA biosynthesis is not essential for the flg22-triggered H_2O_2 over-accumulation in the *nsl1* mutants. We next generated and examined *nsl1 rbohD* double mutants. The increased H_2O_2 accumulation upon flg22 treatment at 48 h after MAMP application was abolished in this line (Figure 5(b)), indicating that the MAMP-induced ROS accumulation in the *nsl1* mutants prior to the MAMP-induced cell death depends on the NADPH oxidase RBOHD (Torres *et al.*, 2002). By contrast, the flg22-induced lesion formation in the *nsl1 rbohD* mutant was the same as in the *nsl1* mutants (Figure 5(a)). Collectively, these results indicate that flg22 elicits cell death and increased ROS generation in the *nsl1* mutants and that SID2-dependent SA biosynthesis, but not RBOHD-dependent ROS accumulation, is critical for the MAMP-triggered cell death.

As *nsl1* plants exhibited a hydrogen peroxide over-accumulation phenotype and lesion formation upon flg22 treatment, we also tested *nsl1* plants for other MAMP-triggered cellular responses. It is known that flg22 rapidly (within minutes) activates mitogen-activated protein kinases (MAPKs) such as MPK3 and MPK6 (Asai *et al.*, 2002). We investigated this early MAMP response and found that the *nsl1-3* and *nsl1-4* mutations had no apparent effects on the timing of MAPK activation (Figure 5(c)). flg22 also induces PMR4/GSL5-dependent callose deposition in Arabidopsis (Jacobs *et al.*, 2003; Nishimura *et al.*, 2003; Clay *et al.*, 2009). The *nsl1-3* and *nsl1-4* mutants accumulated callose upon flg22 treatment as did WT plants (Figure S6). Clay *et al.* (2009) reported that in Arabidopsis flg22-induced callose deposition is dependent on PEN2-mediated IG-metabolism. *PEN2* encodes a myrosinase that hydrolyzes 4-

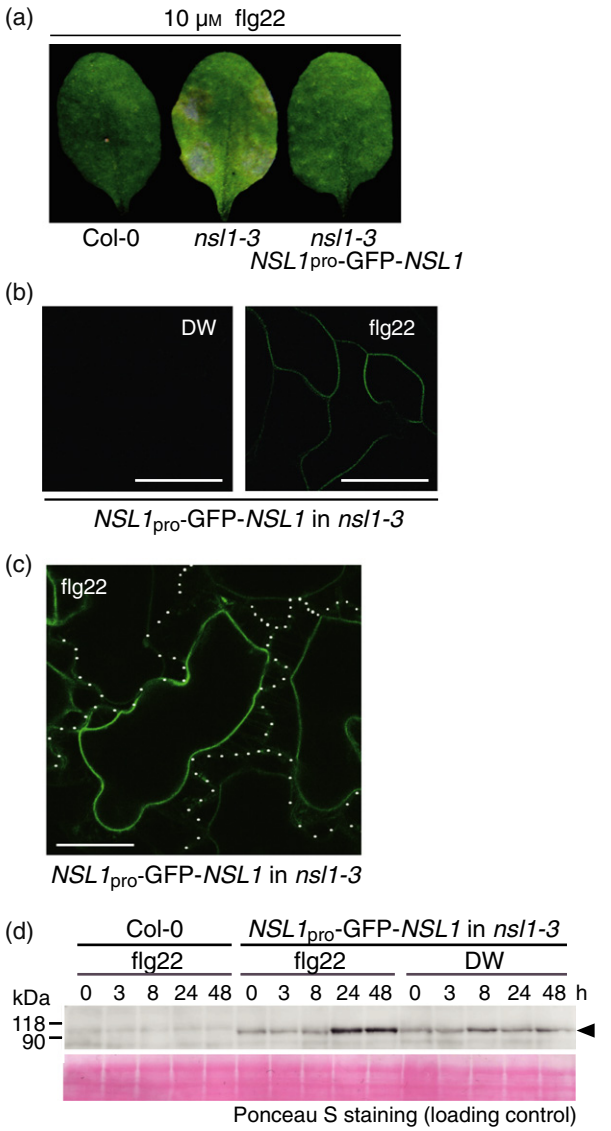

Figure 3. flg22-Induced expression of NSL1 and its cellular localization.
(a) Expression of *GFP–NSL1* under its native promoter complements the *nsl1* phenotype. The flg22 (10 μM) solution was dropped on the leaf surface of the tested Arabidopsis lines, and the plants were incubated for 4 days.
(b) Localization of GFP–NSL1 under the MAMP treatment. flg22 was administered to the transgenic *nsl1* line expressing GFP–NSL1 under its native promoter. A photograph was taken at 18 hpt of flg22. Bars = 50 μm. DW, distilled water was treated.
(c) Plasmolysis assay toward the transgenic line expressing GFP–NSL1. The *nsl1* line expressing GFP–NSL1 was treated with flg22 for 24 h and subjected to the plasmolysis treatment. White dot lines represent boundaries of each epidermal cell. Bar = 30 μm.
(d) Immunoblot of GFP–NSL1 fusion protein probed with the anti-GFP antibody. Arrowhead indicates GFP–NSL1 protein. flg22 enhanced GFP–NSL1 accumulation at 24 and 48 hpt.

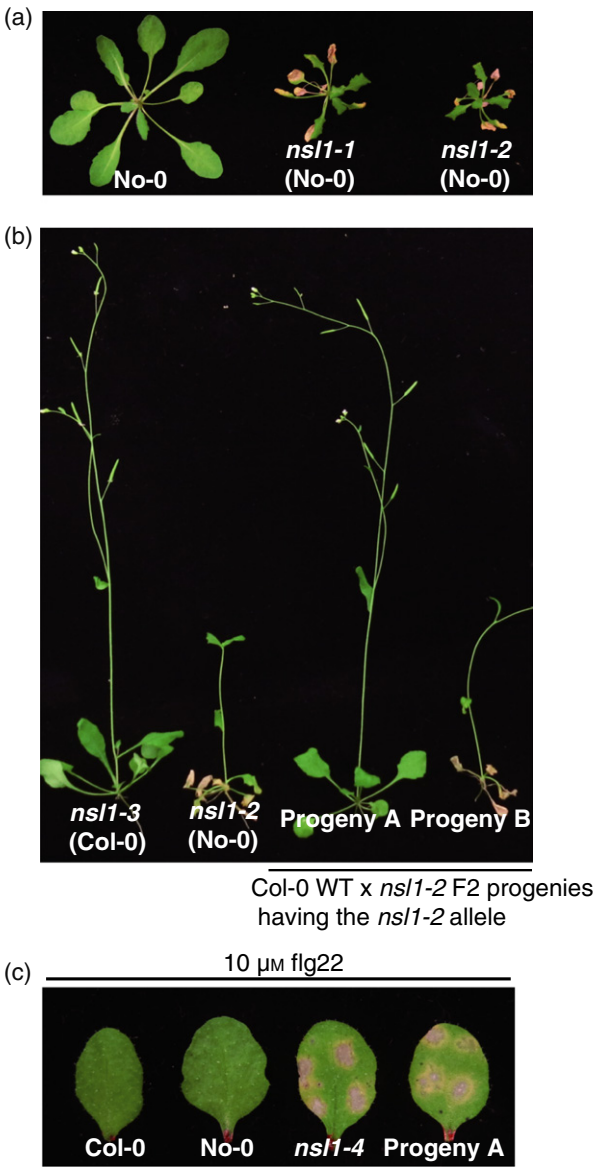

Figure 4. Physiological effects of the *nsl1* insertion mutations are changed in the background of a distinct accession.
(a) The phenotype of the *nsl1* mutants in No-0 background. Each plant was grown for 25 days without MAMP treatment.
(b) The phenotypic variation among F2 progenies carrying the *nsl1-2* allele generated from cross between the *nsl1-2* mutant and the wild-type (WT) Col-0. Among F2 progenies derived from cross of the *nsl1-2* with Col-0, multiple *nsl1-2* lines were identified. Although a part of the identified *nsl1-2* F2 progenies exhibit the growth reduction with yellowish lesions in the absence of MAMP treatment (ex. progeny B), the other *nsl1-2* F2 progenies did not exhibit any growth reduction and lesions the same as WT (ex. progeny A).
(c) flg22 treatment induced PCD in the *nsl1-2* F2 progenies showing the WT growth phenotype. flg22 at 10 μM was spotted in each tested plant and treated plants are incubated for 4 days. The *nsl1-2* F2 progenies showing the WT growth phenotype (progeny A) developed lesions on the flg22-treated area, which is quite similar to the phenotype of the *nsl1-4* mutant of Col-0.

methoxyindol-3-ylmethyl glucosinolate (4MI3G) as *in planta* substrate for antifungal defense responses (Bednarek *et al.*, 2009; Clay *et al.*, 2009). We generated the *nsl1-4 pen2* double mutant and confirmed that callose deposition in *nsl1* was suppressed by the *pen2* mutation (Figure S6). This suggests that there are no obvious effects of *nsl1* on the flg22-induced callose deposition pathway. The *nsl1 sid2* mutant accumulated callose upon flg22 treatment as did

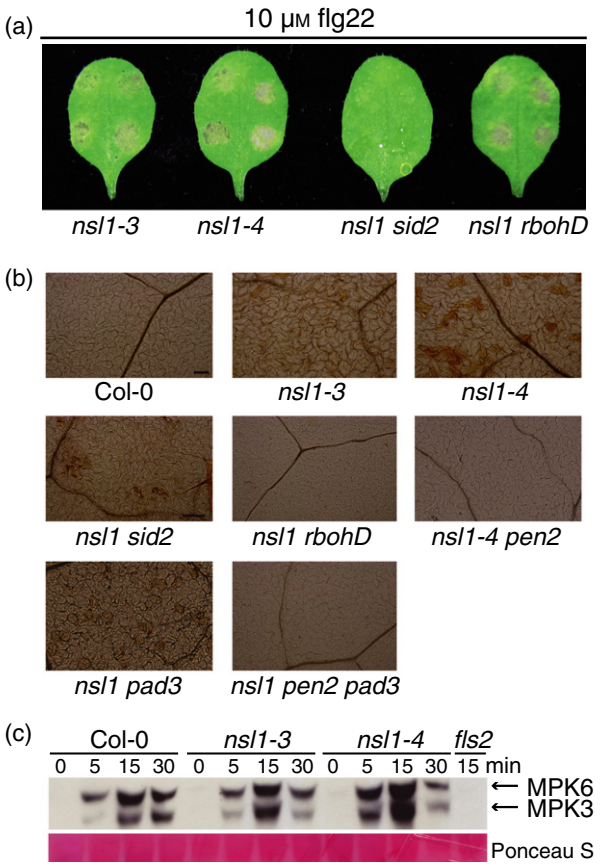

Figure 5. Contribution of SA, ROS and MAPK to the flg22-triggered PCD in the *nsl1* mutants.
(a) *sid2* abrogates flg22-triggered PCD in the *nsl1* mutant. flg22 at 10 μM was dropped on the leaf surface of tested plants. The plants were incubated for 4 days.
(b) H_2O_2 accumulation in *nsl1* lines. Leaves of tested plants were dropped with flg22 at 10 μM, incubated for 48 h and stained with DAB to detect H_2O_2. Bar = 200 μm.
(c) MAPK activation in Arabidopsis seedlings upon application of 1 μM flg22 for the indicated times. The positions of active MPK3 and MPK6 forms are indicated (right).

the *nsl1* single mutants of Col-0 (Figure S6), demonstrating that callose deposition can be uncoupled from cell death in flg22-treated *nsl1* plants.

Pathogen-triggered Trp metabolism is involved in flg22-induced PCD in *nsl1* mutants

We noticed that the *pen2* mutation largely suppresses flg22-induced lesion formation in the *nsl1* mutants of the accession Col-0 (Figure 6(a)). The *nsl1 pen2* double mutants occasionally showed weak leaf lesions upon flg22 treatment, whereas *nsl1* single mutants invariably exhibited severe lesion formation. Importantly, the *pen2* mutation also abolished *Co*-triggered cell death in *nsl1* plants (Figure S7). CYP81F2 P450 monooxygenase is essential for the pathogen-inducible accumulation of 4MI3G, the biologically relevant substrate of PEN2 myrosinase (Bednarek *et al.*, 2009; Clay *et al.*, 2009). We further generated the *nsl1-3 cyp81F2-2* double mutant and found that *CYP81F2* is indeed essential for the flg22-triggered cell death in the *nsl1* background (Figure 6(a)). These results indicate that products of the CYP81F2/PEN2 pathway are engaged in the *nsl1*-mediated cell death response. In a trypan blue vital staining assay we detected dye precipitate in leaf cells in the lesion area of flg22-treated *nsl1* mutants at 96 hpt, whereas only faint retention of the dye was seen in *nsl1 sid2, nsl1 pen2,* and *nsl1 cyp81F2* genotypes (Figure 6(b)). We thus conclude that the CYP81F2/PEN2 pathway as well as the SA pathway is involved in the MAMP-triggered cell death in the absence of functional NSL1 protein.

To directly assess the activity of the PEN2-dependent metabolic pathway in *nsl1* plants, we monitored accumulation levels of its end products, (i) raphanusamic acid (RA) and (ii) indol-3-ylmethylamine (I3A) derived from indol-3-ylmethyl glucosinolate (I3G), and (iii) 4-*O*-β-D-glucosyl-indol-3-yl formamide (4OGlcI3F) derived from 4-methoxy-indol-3-ylmethyl glucosinolate (4MI3G), in leaf extracts (Bednarek *et al.*, 2009; Bednarek, 2012; Lu *et al.*, 2015) (Figures 7(a) and S8). Accumulation of these compounds increased markedly in the *nsl1-3* and *nsl1-4* mutants as compared with Col-0 at both 48 and 72 h after flg22 application, whereas their low-level constitutive accumulation in *nsl1* was comparable to that observed in WT (Figure 7(a)). These results indicate that the lack of functional NSL1 enhances the flg22-induced accumulation of PEN2 pathway end products, including RA, I3A and 4OGlcI3F (Figure S8; Bednarek *et al.*, 2009; Lu *et al.*, 2015).

IGs, which are PEN2 substrates, are derived from Trp, an aromatic amino acid that in Arabidopsis serves also as precursor of other pathogen-inducible metabolites, including camalexin and indol-3-carboxylic acid derivatives (I3CAs) (Bednarek, 2012; Bednarek *et al.*, 2005) (Figure S8). Camalexin is an antifungal metabolite, regarded as Arabidopsis phytoalexin, and is produced by a relatively well characterized pathway involving the cytochrome P450 monooxygenases PAD3 (Phytoalexin Deficient 3) (Zhou *et al.*, 1999). We monitored accumulation levels of camalexin and I3CAs upon flg22 treatment, which both increased markedly in the *nsl1* mutants compared to WT (Figure 7(a)).

The increased camalexin accumulation suggested that this antifungal metabolite might be linked to the flg22-induced PCD in the *nsl1* plants. To test this we generated and examined *nsl1 pad3* double and *nsl1 pen2 pad3* triple mutants. The *nsl1 pad3* line developed a cell death phenotype; however, leaf lesions were weaker in this line compared to *nsl1* plants (Figure S9(a)). Although *nsl1 pen2* leaves occasionally developed weak lesions upon flg22 treatment, the *nsl1 pen2 pad3* triple mutant completely failed to mount a cell death response upon flg22 treatment

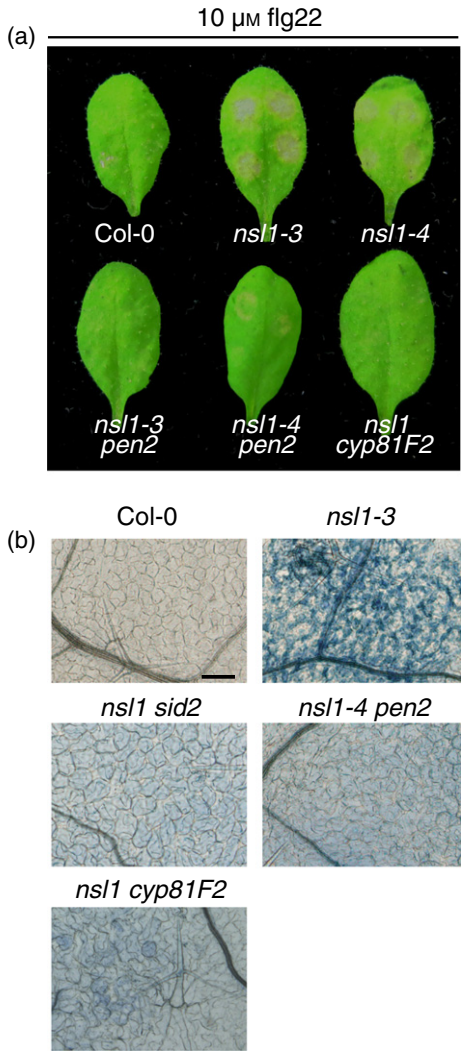

Figure 6. Involvement of PEN2- metabolic pathway in flg22-induced PCD in the *nsl1* mutant.
(a) Both *PEN2* and *CYP81F2* are required for the flg22-induced PCD of the *nsl1* mutant. flg22 at 10 μM was dropped on the tested plants. In contrast to the *nsl1* mutants, the *nsl1 pen2* and *nsl1 cyp81F2* double mutants did not exhibit the lesion phenotype.
(b) Trypan blue staining. Each flg22-treated plant was subjected to trypan blue staining at 96 hpt. At that time when lesions were visible in *nsl1* mutants, shrunken dead cells, strongly stained with the dye, were detected in the *nsl1* mutants but not in the other plant lines. Bar = 400 μm.

(Figure S9(b)). These findings suggest that the phytoalexin camalexin is involved in the cell death of flg22-treated *nsl1* mutants, although the PEN2-dependent metabolites play a major role. Taken together, our findings demonstrate that two branches of Trp-derived secondary metabolism together with SA biosynthesis are needed for MAMP-triggered lesion formation in *nsl1* mutants.

Additionally, in contrast to *nsl1* and *nsl1 sid2* plants, ROS accumulation at 48 h after flg22 application was abrogated in the *nsl1 pen2* and *nsl1 pen2 pad3* plants (Figure 5(b)). The ROS accumulation in the *nsl1 pad3* plants was similar to the *nsl1* plants (Figure 5(b)). Thus, the enhanced accumulation of the Trp-derived and PEN2-dependent metabolites is involved in triggering ROS accumulation in the *nsl1* mutants upon MAMP treatment, whereas the SA biosynthesis is not essential for this phenomenon.

Increased accumulation of SA in *nsl1* depends on Trp metabolism

Next we examined the relationship between Trp metabolism and SA biosynthesis in *nsl1*-dependent leaf cell death. Although SA levels in non-challenged *nsl1-3* and *nsl1-4* leaves were similar to those in WT, SA accumulation in the *nsl1* mutants at 24 h after flg22 application was increased compared to WT (Figure 7(b)). These results suggest that MAMP treatment triggered SA biosynthesis in *nsl1* plants. Because *nsl1 sid2* mutants fail to activate cell death upon flg22 treatment, the observed SA accumulation is needed for flg22-induced lesion formation in a *nsl1* background. Remarkably, the *pen2 pad3* double mutation caused complete abrogation of SA accumulation in the *nsl1* background (Figure 7(b)). Together with our aforementioned genetic evidence, the finding suggests that Trp-derived metabolites are needed for SA accumulation in flg22-treated *nsl1* mutants. These results reveal an unexpected molecular link between antimicrobial metabolites and the SA defense phytohormone pathway.

To further investigate this link, we tested the effects of the *sid2* mutation on Trp metabolism in the *nsl1* background. The accumulation of the end products of the PEN2 pathway (I3A and RA) in the *nsl1* mutant was not decreased by the *sid2* mutation (Figure 7(c)). By contrast, the elevated levels of camalexin and I3CAGlc were partially suppressed in the *nsl1 sid2* plants (Figure 7(c)), implying the involvement of SA in the accumulation of these metabolites. As discussed above, PEN2 (but not PAD3) is critical for MAMP-triggered cell death in *nsl1* plants (Figures 6 and S9). Collectively, these findings suggest that the increased accumulation of PEN2-related metabolites activates SA biosynthesis and signaling in the *nsl1* plants of Col-0 upon MAMP treatment, which leads to a genetically determined cell death in this mutant.

DISCUSSION

Unlike ETI, MTI is normally uncoupled from host cell death responses. ETI displays amplified and sustained immune responses compared with MTI, suggesting that quantitative rather than qualitative differences account for the activation of ETI-associated cell death (Tsuda and Katagiri, 2010). However, it remains unclear whether an amplified MTI is able to trigger cell death via the same or different genetic programs as in ETI. Here we have shown that leaf surface treatment with peptide MAMPs induces a genetically defined cell death in the Arabidopsis *nsl1* mutants (Col-0

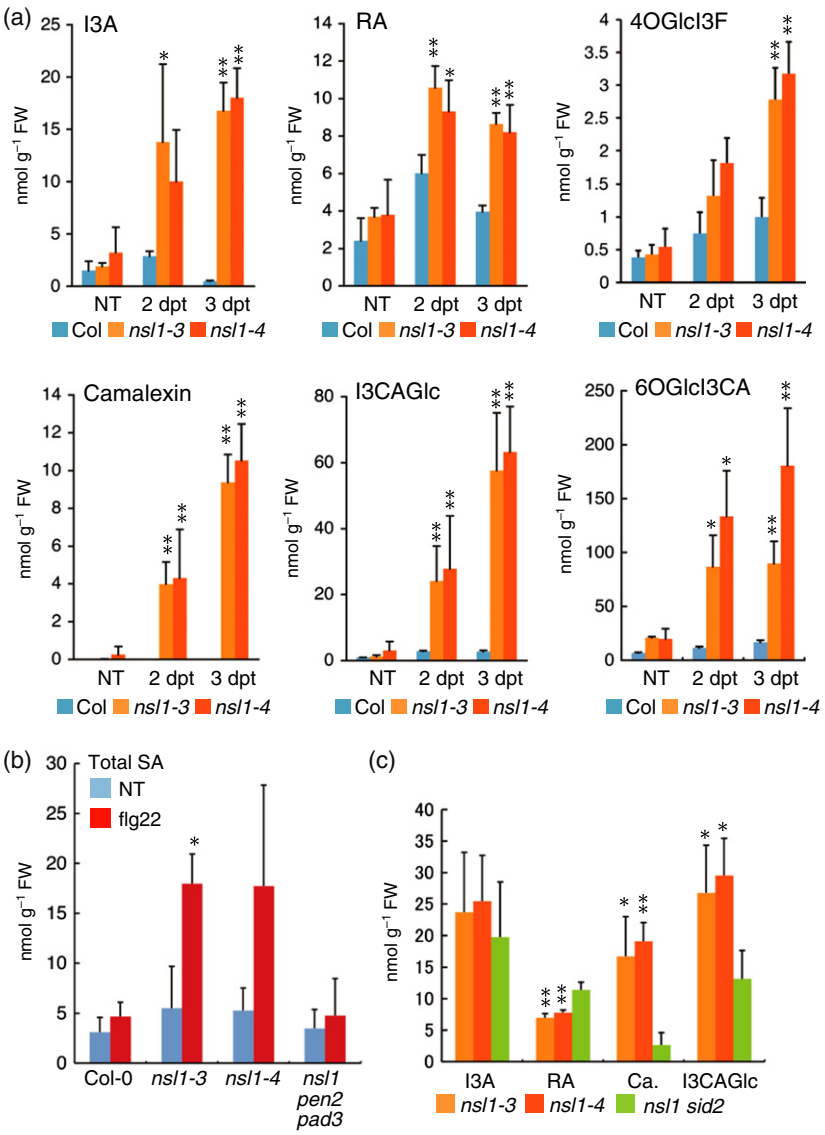

Figure 7. Accumulation of Trp-derived metabolites and salicylic acid in the *nsl1* mutants sprayed with flg22 (10 μM).
(a) Accumulation of Trp-derived secondary metabolites at the indicate time points after flg22 treatment.
(b) Total salicylic acid levels in *nsl1* mutants 24 h after flg22 application.
(c) The effect of *sid2* mutation on accumulation of Trp-derived metabolites in the *nsl1* background.
The means and standard deviations (SDs) were calculated from three independent experiments. In each experiment single samples have been collected per genotype in each time point. The statistical significance of differences between means was determined on log-transformed data by Tukey test. $^{**}P < 0.01$, $^{*}P < 0.05$ [comparison of Col-0 with *nsl1* mutants in Figure 7(a, b); comparison of *nsl1* mutants with *nsl1 sid2* mutant in Figure 7(c)].
NT: nontreated control plants, I3A: indol-3-ylmethylamine; RA: raphanusamic acid; 4OGlcI3F: 4-*O*-β-D-glucosyl-indol-3-yl formamide. I3CAGlc: glucose ester of indole-3-carboxylic acid; 6OGlcI3CA: 6-*O*-β-glucosyl-indole-3-carboxylic acid, Ca: camalexin.

background) that are depleted in an MACPF domain protein, thereby revealing a potential MAMP-triggered PCD.

The relationship between MTI and ETI described above prompts the question whether MTI responses in *nsl1* plants are amplified compared with those in WT. It has been reported that flg22 triggers the accumulation of SA as well as ROS in Arabidopsis WT (Tsuda *et al.*, 2008). We found that the *nsl1* mutations enhanced these MTI outputs (Figures 5(b) and 7 (b)), supporting the notion that MTI responses are enhanced in *nsl1* plants. We found that enhanced activation of SA biosynthesis is critical for MAMP-triggered PCD in *nsl1* (Figure 5(a)). It has been reported that ETI, triggered by the bacterial effector AvrRpt2, accompanies sustained activation of MAPK signaling to regulate SA-responsive genes independently of SA, and this compensatory relationship between MAPKs and SA signaling is thought to confer robustness to ETI compared with MTI (Tsuda *et al.*, 2013). In contrast, *nsl1* plants did not exhibit sustained activation of MPK3 and MPK6 upon MAMP treatment, at least early after MAMP treatment (within 30 min; Figure 5(c)), suggesting that in the absence of NSL1 enhanced SA biosynthesis plays a major role for MAMP-triggered PCD without sustained MAPK activation.

Our genetic analysis demonstrated that MAMP-triggered PCD in *nsl1* plants is not only dependent on SA biosynthesis, but also on Trp-derived metabolites (Figure 6). Further analyses suggested that an increased production of these secondary metabolites activated SA biosynthesis (Figure 7(b)), thereby revealing a previously unsuspected role of Trp-derived metabolites in the regulation of the SA defense phytohormone pathway and PCD. DAB staining assays indicated that flg22 triggers ROS generation in both *nsl1* and *nsl1 sid2* plants, but not in *nsl1 pen2* plants, at

48 h after the treatment (Figure 5(b)). This suggests that the accumulation of PEN2-related metabolites in *nsl1* plants is essential for MAMP-triggered PCD and that subsequent SA accumulation amplifies the PCD response.

Comparison of *nsl1 pen2* with the *nsl1 pad3* mutant showed that the PEN2-dependent products of IG hydrolysis play a major role in *nsl1* PCD, whereas camalexin had a minor role (Figure S9). In this context it is notable that PEN2, but not PAD3, was previously shown to be required for flg22-induced callose deposition in Arabidopsis (Clay *et al.*, 2009). We found that SA signaling is critical for flg22-induced PCD (Figure 5(a)), but not for flg22-triggered callose deposition in *nsl1* plants (Figure S5). This finding suggests that PEN2-dependent metabolites can act as signal molecules that activate the SA pathway leading to PCD, especially in the absence of NSL1, probably uncoupled from the flg22-induced callose deposition pathway. Furthermore, a recent report suggested that *PEN1, PEN2,* and *PEN3* contribute to effector-triggered PCD upon challenge with bacterial or oomycete pathogens, implying a general role of PEN2-dependent metabolites in defense-related PCD forms (Johansson *et al.*, 2014). In contrast to the end products of the PEN2 pathway (I3A and RA), the accumulation of camalexin and I3CAs in *nsl1* plants was partially suppressed by *sid2,* suggesting that SA contributes to an increased production of these metabolites (Figure 7(c)). Similarly, the accumulation of camalexin, but not I3A and RA, is strongly induced by *Cg* invasion in Arabidopsis (Hiruma *et al.*, 2013). These data point to a distinct regulatory relationship between the PEN2-related metabolic pathway and the camalexin/I3CA pathway.

We identified the *nsl1* mutants by screening with *C. orbiculare* (*Co*), a nonadapted pathogen on Arabidopsis (Figure 1(a)). In addition, we showed that a closely related nonadapted *Colletotrichum* species, *C. gloeosporioides* (*Cg*), also triggered PCD in *nsl1* without successful fungal invasion (Figure 1(c, d)). The analysis on the *nsl1 cerk1* mutants suggested that CERK1-dependent chitin recognition is not essential for *Co*-triggered PCD (Figure 2(d)). These findings indicate that *Colletotrichum* species have unidentified MAMP(s) that trigger PCD in the *nsl1* mutants of Arabidopsis accession Col-0. We reported that entry attempts of *Co* and *Cg* are terminated in Arabidopsis Col-0 by pre-invasive nonhost resistance that requires CYP81F2 and PEN2 (Shimada *et al.*, 2006; Hiruma *et al.*, 2010). Thus, the pre-invasive nonhost resistance of Arabidopsis might be triggered by the same unidentified MAMP(s) that induces PCD in the *nsl1* mutants. Consequently, the *nsl1* mutants could be utilized as tool to identify the unidentified MAMP(s) of *Colletotrichum* species.

In the animal complement system, MACPF domain proteins are assembled to form pores in the membranes of invasive bacteria, which help to kill them as a part of the immune response (Rosado *et al.*, 2008; Kondos *et al.*, 2010; McCormack *et al.*, 2013). In contrast, upon MAMP treatment, Arabidopsis NSL1 localizes to the plasma membrane of host cells without killing them (Figure 3(b, c)), implying that NSL1 has molecular functions distinct from those of the animal MACPF proteins in immunity or that pore formation requires an additional cue. The other regions of NSL1 are conserved in higher plants, but distinct from those of animal MACPF proteins (Gilbert *et al.*, 2013). One possibility is that putative NSL1 pore formation is regulated by plant-unique regions flanking the MACPF domain or by other plant factors, similar to the inhibitory effect of CD59 on human MACPF proteins of the complement system (Huang *et al.*, 2006). Here we indicate that the phenotypic difference of the *nsl1-3* and *nsl1-4* mutants (Col-0 background) from *nsl1-1* and *nsl1-2* mutants (No-0 background) depends entirely on natural genetic variation of other loci in their respective parental accessions and not on mutant allele-specific differences (Figures 4 and S4). Interestingly, the *nsl1-4* mutation locates to the plant-unique region close to the C-terminus of NSL1, suggesting that this region is critical for protein function(s) (Figures 1(b) and S1). Also, the *nsl1-3* mutation changes Gly_{109} to an Arg and this Gly residue is conserved in all Arabidopsis NSL1 homologs (At4 g24290, At1g29690, and At1g14780; Figure S1). These findings will be useful for future structural and functional analyses of plant MACPF domain proteins that are distinct from animal MACPF domain proteins.

Why do the *nsl1* mutant alleles cause severe dwarfism phenotypes in the No-0 but not in the Col-0 genetic background? One possibility is that NSL1 is guarded by an unidentified intracellular NLR-type immune sensor present in No-0 and absent in Col-0. For example, the accelerated cell death 11 (*acd11*) 'lesion mimic' mutant of Arabidopsis exhibits autoimmune phenotypes such as constitutive defense responses and cell death without pathogen perception and dominant negative mutations in the TIR-type NLR *LAZ5* suppress *acd11* death (Palma *et al.*, 2010). Similarly, a genetic screen for suppressors of the autoimmune phenotype of Arabidopsis *mkk1 mkk2* mutants, in which the MAMP-induced MAP kinase cascade is disrupted, revealed the NLR *SUMM2* (Zhang *et al.*, 2012). A truncated Arabidopsis NLR Protein, TIR-NBS2, was recently shown to be required for activated defense responses in the *exo70B1* mutant, encoding an evolutionary conserved component of the exocyst complex that serves a critical role in plant secretory pathways (Zhao *et al.*, 2015). Common features of 'autoimmunity' in *nsl1, exo70B1, acd11* and *mkk1 mkk2* plants are constitutive defense responses, dwarfism and/or leaf necrosis. However, mutations in *RAR1* and *SGT1,* which are needed for the function of a subset of NLR-type immune receptors, have no impact on the *nsl1* phenotype of No-0 (Noutoshi *et al.*, 2006; Shirasu, 2009). Also, there is a possibility that natural variation of genes involved in the

biosynthesis of IGs in Col-0 and No-0 accessions might affect the *nsl1* phenotype. Interestingly, an insertion mutation in *At1g29690,* a close homolog of *NSL1,* resulted in growth retardation and spontaneous leaf cell death in the Col-0 background (Morita-Yamamuro *et al.*, 2005), resembling the *nsl1* mutants of No-0, and suggesting overall related but accession-dependent functions for each MACPF domain protein. These findings and the *nsl1* mutant alleles described in the present study provide genetic tools and a genetic framework to examine in future work the biochemical function(s) of plant MACPF domain proteins in plant defense to pathogens.

EXPERIMENTAL PROCEDURES

Screening of Arabidopsis mutants that form lesions after *C. orbiculare* inoculation

We purchased EMS-mutagenized M2 seeds of Col-0 from Lehle Seeds (Round Rock, TX, USA). Plants approximately 4 weeks old were spray-inoculated with a conidial suspension (~5×10^5 conidia/mL) of *C. orbiculare* (*Co*). Inoculated plants were placed in a growth chamber at 25°C with a cycle of 16 h of light and 8 h of dark and maintained at 100% relative humidity. The lesion phenotype of the inoculated M2 plants was investigated at 5–7 days post inoculation (dpi). Col-0 did not exhibit any lesions after the *Co* inoculation.

Plant lines and growth

Arabidopsis thaliana accession Col-0 was used as the WT. *pen2-1, pen2-2* (Lipka *et al.*, 2005), *pen3-1* (Stein *et al.*, 2006), *cyp81F2-2* (Bednarek *et al.*, 2009), *atrbohD* (Torres *et al.*, 2002), *fls2* (Heese *et al.*, 2007), *sid2-2* (*eds16*) (Dewdney *et al.*, 2000), *pad3-1*(Zhou *et al.*, 1999), *pad4-1* (Glazebrook and Ausubel, 1994), *nsl1-1* and *nsl1-2* (Noutoshi *et al.*, 2006) and *cerk1-2* (Miya *et al.*, 2007) mutants were described earlier. Plants were sown on rockwool, treated at 4°C in the dark for 2 days, and grown at 25–26°C with 16 h of illumination per day in nutrient medium.

Fungal materials

The *Co* WT strain 104-T (MAFF 240422), a pathogen of cucumber, is a stock culture of the Laboratory of Plant Pathology, Kyoto University. *Colletotrichum gloeosporioides* S9275 (*Cg*), a pathogen of mulberry, was provided by Shigenobu Yoshida (National Institute for Agro-Environmental Sciences, Japan). Cultures of the fungal isolates were maintained on 3.9% (w/v) potato dextrose agar medium (PDA; Difco, Detroit, MI, USA) at 24°C in the dark. Conidia of *Cg* were prepared from fungal culture grown with a cycle of 16 h of black light and 8 h dark.

MAMP treatment

The MAMP peptide dissolved in water was administered to Arabidopsis plants by spotting 5-μL drops on each leaf. Treated plants were then placed in a growth chamber at 25°C with a cycle of 16 h of light and 8 h of dark, and maintained at 100% relative humidity.

Generation of double or triple mutants by crossing

By crossing *nsl1-3* and *nsl1-4* with the mutants described above, we generated double or triple mutants as following; *nsl1-3 cerk1-2, nsl1-4 sid2-2, nsl1-3 rbohD, nsl1-3 pad4-1, nsl1-3 pen2-1, nsl1-4 pen2-1, nsl1-3 pen2-2, nsl1-3 cyp81F2-2, nsl1-4 pad3-1,* and *nsl1-4 pen2-1 pad3-1.* All of the mutant lines except *pen2-1* (Col-0 *gl1* background) were in the Col-0 background. The *nsl1-2* mutants (No-0 background) were crossed with Col-0 WT. The *nsl1-4* mutant (Col-0 background) was also crossed with No-0 WT. The *nsl1-3, nsl1-4, pen2-1, pen3-1,* and *pad4-1* mutations were checked with the corresponding specific primers for derived cleaved amplified polymorphic sequence (dCAPS) markers found by the dCAPS Finder 2.0 (http://helix.wustl.edu/dcaps/dcaps/dcaps.html). Both types of polymerase chain reaction (PCR) products (WT and mutant) were cleaved with corresponding enzymes. The *pen2-2, cyp81F2-2, atrbohD* and the *nsl1-2* mutants had T-DNA or transposon insertions, and the insertions were checked by PCR using corresponding gene-specific primers and the insertion type-specific primers. The fast neutron-generated *sid2-2* mutation was also checked by corresponding specific primers. The *pad3-1* mutation was checked by sequencing using the listed primers. Table S1 shows a list of primers used in genotyping the mutations.

Analyses of Trp metabolites and salicylic acid

Plant samples (100–200 mg fresh weight for each sample) were collected at 0, 48, and 72 h (Trp-metabolites) or 24 h (SA) after spray inoculation with flg22 (10 μM) and frozen in liquid nitrogen. Extraction and HPLC analysis of Trp derivatives was performed as previously described (Bednarek *et al.*, 2009; Lu *et al.*, 2015). Extraction and analysis of total SA followed the protocol of Bartsch *et al.* (2006). Each line was tested in three independent experiments. In each experiment single samples have been collected per genotype in each time point.

Experimental methods for DAB staining, confocal microscopy, TILLING, trypan blue staining, western blot analysis, assays of MAMP-induced responses, and plasmid construction are described in Methods S1.

ACKNOWLEDGEMENTS

We thank Jeffery Dangl (University of North Carolina, USA: *atrbohD*), Volker Lipka (Georg-August-University Goettingen, Germany, *sid2-2*), Takashi Kuromori (RIKEN CSRS, Japan, *nsl1-1* and *nsl1-2*), Naoto Shibuya (Meiji University, Japan, *cerk1-2*), the ABRC (Ohio State University, USA: *pad3-1, pad4-1*) for providing seeds. This work was supported in part by Grants-in-Aid for Scientific Research (15H05780, 15H04457 and 20380027) from the Ministry of Education, Culture, Sports, Science and Technology of Japan; by Asahi Glass Foundation, and by the Science and Technology Research Promotion Program for Agriculture, Forestry, Fisheries and Food industry (to Y.T.). Work in the Paweł Bednarek laboratory was supported with an EMBO Installation Grant. We thank Mika Kojima, Hiroe Utsushi and Małgorzata Zielińska for technical assistance.

CONFLICT OF INTEREST

The authors have no conflict of interests to declare.

SUPPORTING INFORMATION

Additional Supporting Information may be found in the online version of this article.

Figure S1. Alignments of the *A. thaliana* NSL1 sequence with those of the other three proteins of *A. thaliana* having a MACPF domain.

Figure S2. Application of 1 μM flg22 and elf18 on the *nsl1* plants.

Figure S3. Analysis of the transgenic *nsl1* lines expressing GFP–NSL1 where *Co* was inoculated.

Figure S4. The *nsl1-4* mutation causes the growth retardation and spontaneous necrotic lesions in Arabidopsis plants.

Figure S5. Mutations of genes involved in SA signaling reduced the *nsl1*-PCD under the both MAMP and pathogen treatments.

Figure S6. flg22-triggered callose deposition is not altered by the *nsl1* mutation.

Figure S7. *pen2* mutations suppressed the *nsl1*- PCD under the pathogen treatment.

Figure S8. A model of Trp metabolism pathways involving PEN2, CYP81F2 and PAD3.

Figure S9. Contribution of camalexin to flg22-triggered PCD.

Table S1. Primers used in this study.

Methods S1. Supplementary methods.

REFERENCES

Asai, T., Tena, G., Plotnikova, J., Willmann, M.R., Chiu, W.L., Gomez-Gomez, L., Boller, T., Ausubel, F.M. and Sheen, J. (2002) MAP kinase signalling cascade in Arabidopsis innate immunity. *Nature*, **415**, 977–983.

Bartsch, M., Gobbato, E., Bednarek, P., Debey, S., Schultze, J.L., Bautor, J. and Parker, J.E. (2006) Salicylic acid-independent ENHANCED DISEASE SUSCEPTIBILITY1 signaling in Arabidopsis immunity and cell death is regulated by the monooxygenase FMO1 and the nudix hydrolase NUDT7. *Plant Cell*, **18**, 1038–1051.

Bednarek, P. (2012) Sulfur-containing secondary metabolites from *Arabidopsis thaliana* and other *Brassicaceae* with function in plant immunity. *Chem. Bio. Chem.* **13**, 1846–1859.

Bednarek, P., Schneider, B., Svatos, A., Oldham, N.J. and Hahlbrock, K. (2005) Structural complexity, differential response to infection, and tissue specificity of indolic and phenylpropanoid secondary metabolism in *Arabidopsis* roots. *Plant Physiol.* **138**, 1058–1070.

Bednarek, P., Pislewska-Bednarek, M., Svatos, A. *et al.* (2009) A glucosinolate metabolism pathway in living plant cells mediates broad-spectrum antifungal defence. *Science*, **323**, 101–106.

Boller, T. and Felix, G. (2009) A renaissance of elicitors: perception of microbe-associated molecular patterns and danger signals by pattern-recognition receptors. *Annu. Rev. Plant Biol.* **60**, 379–406.

Clay, N.K., Adio, A.M., Denoux, C., Jander, G. and Ausubel, F.M. (2009) Glucosinolate metabolites required for an *Arabidopsis* innate immune response. *Science*, **323**, 95–101.

Dewdney, J., Reuber, T.L., Wildermuth, M.C., Devoto, A., Cui, J., Stutius, L.M., Drummond, E.P. and Ausubel, F.M. (2000) Three unique mutants of *Arabidopsis* identify *eds* loci required for limiting growth of a biotrophic fungal pathogen. *Plant J.* **24**, 205–218.

Dodds, P.N. and Rathjen, J.P. (2010) Plant immunity: towards an integrated view of plant-pathogen interactions. *Nat. Rev. Genet.* **11**, 539–548.

Gan, P., Ikeda, K., Irieda, H., Narusaka, M., O'Connell, R.J., Narusaka, Y., Takano, Y., Kubo, Y. and Shirasu, K. (2013) Comparative genomic and transcriptomic analyses reveal the hemibiotrophic stage shift of *Colletotrichum* fungi. *New Phytol.* **197**, 1236–1249.

Gilbert, R.J., Mikelj, M., Dalla Serra, M., Froelich, C.J. and Anderluh, G. (2013) Effects of MACPF/CDC proteins on lipid membranes. *Cell. Mol. Life Sci.* **70**, 2083–2098.

Glazebrook, J. and Ausubel, F.M. (1994) Isolation of phytoalexin-deficient mutants of *Arabidopsis thaliana* and characterization of their interactions with bacterial pathogens. *Proc. Natl Acad. Sci. USA*, **91**, 8955–8959.

Heath, M.C. (2000a) Hypersensitive response-related death. *Plant. Mol. Biol.* **44**, 321–334.

Heath, M.C. (2000b) Nonhost resistance and nonspecific plant defenses. *Curr. Opin. Plant Biol.* **3**, 315–319.

Heese, A., Hann, D.R., Gimenez-Ibanez, S., Jones, A.M., He, K., Li, J., Schroeder, J.I., Peck, S.C. and Rathjen, J.P. (2007) The receptor-like kinase SERK3/BAK1 is a central regulator of innate immunity in plants. *Proc. Natl Acad. Sci. USA*, **104**, 12217–12222.

Hiruma, K., Fukunaga, S., Bednarek, P., Pislewska-Bednarek, M., Watanabe, S., Narusaka, Y., Shirasu, K. and Takano, Y. (2013) Glutathione and tryptophan metabolism are required for Arabidopsis immunity during the hypersensitive response to hemibiotrophs. *Proc. Natl. Acad. Sci. USA*, **110**, 9589–9594.

Hiruma, K., Onozawa-Komori, M., Takahashi, F., Asakura, M., Bednarek, P., Okuno, T., Schulze-Lefert, P. and Takano, Y. (2010) Entry mode-dependent function of an indole glucosinolate pathway in Arabidopsis for nonhost resistance against anthracnose pathogens. *Plant Cell*, **22**, 2429–2443.

Huang, Y., Qiao, F., Abagyan, R., Hazard, S. and Tomlinson, S. (2006) Defining the CD59-C9 binding interaction. *J. Biol. Chem.* **281**, 27398–27404.

Jacobs, A.K., Lipka, V., Burton, R.A., Panstruga, R., Strizhov, N., Schulze-Lefert, P. and Fincher, G.B. (2003) An Arabidopsis callose synthase, GSL5, is required for wound and papillary callose formation. *Plant Cell*, **15**, 2503–2513.

Jirage, D., Tootle, T.L., Reuber, T.L., Frost, L.N., Feys, B.J., Parker, J.E., Ausubel, F.M. and Glazebrook, J. (1999) *Arabidopsis thaliana PAD4* encodes a lipase-like gene that is important for salicylic acid signaling. *Proc. Natl Acad. Sci. USA*, **96**, 13583–13588.

Johansson, O.N., Fantozzi, E., Fahlberg, P., Nilsson, A.K., Buhot, N., Tör, M. and Andersson, M.X. (2014) Role of the penetration-resistance genes *PEN1, PEN2* and *PEN3* in the hypersensitive response and race-specific resistance in *Arabidopsis thaliana*. *Plant J.* **79**, 466–476.

Kondos, S.C., Hatfaludi, T., Voskoboinik, I., Trapani, J.A., Law, R.H., Whisstock, J.C. and Dunstone, M.A. (2010) The structure and function of mammalian membrane-attack complex/perforin-like proteins. *Tissue Antigens*, **76**, 341–351.

Kubo, Y. and Takano, Y. (2013) Dynamics of infection-related morphogenesis and pathogenesis in *Colletotrichum orbiculare*. *J. Gen. Plant Pathol.* **79**, 233–242.

Lipka, V., Dittgen, J., Bednarek, P. *et al.* (2005) Pre- and postinvasion defenses both contribute to nonhost resistance in *Arabidopsis*. *Science*, **310**, 1180–1183.

Lu, X., Dittgen, J., Piślewska-Bednarek, M. *et al.* (2015) Mutant allele-specific uncoupling of PENETRATION3 functions reveals engagement of the ATP-binding cassette transporter in distinct tryptophan metabolic pathways. *Plant Physiol.* **168**, 814–827.

Maekawa, T., Kufer, T.A. and Schulze-Lefert, P. (2011) NLR functions in plant and animal immune systems: so far and yet so close. *Nat. Immunol.* **12**, 817–826.

McCallum, C.M., Comai, L., Greene, E.A. and Henikoff, S. (2000) Targeted screening for induced mutations. *Nat. Biotechnol.* **18**, 455–457.

McCormack, R., de Armas, L., Shiratsuchi, M. and Podack, E.R. (2013) Killing machines: three pore-forming proteins of the immune system. *Immunol. Res.* **57**, 268–278.

Miya, A., Albert, P., Shinya, T., Desaki, Y., Ichimura, K., Shirasu, K., Narusaka, Y., Kawakami, N., Kaku, H. and Shibuya, N. (2007) CERK1, a LysM receptor kinase, is essential for chitin elicitor signaling in Arabidopsis. *Proc. Natl Acad. Sci. USA.*, **49**, 19613–19618.

Morita-Yamamuro, C., Tsutsui, T., Sato, M. *et al.* (2005) The Arabidopsis gene *CAD1* controls programmed cell death in the plant immune system and encodes a protein containing a MACPF domain. *Plant Cell Physiol.* **46**, 902–912.

Navarro, L., Zipfel, C., Rowland, O., Keller, I., Robatzek, S., Boller, T. and Jones, J.D. (2004) The transcriptional innate immune response to flg22. Interplay and overlap with Avr gene-dependent defence responses and bacterial pathogenesis. *Plant Physiol.* **135**, 1113–1128.

Nishimura, M.T., Stein, M., Hou, B.H., Vogel, J.P., Edwards, H. and Somerville, S.C. (2003) Loss of a callose synthase results in salicylic acid-dependent disease resistance. *Science*, **301**, 969–972.

Noutoshi, Y., Kuromori, T., Wada, T., Hirayama, T., Kamiya, A., Imura, Y., Yasuda, M., Nakashita, H., Shirasu, K. and Shinozaki, K. (2006) Loss of *Necrotic Spotted Lesions 1* associates with cell death and defence responses in *Arabidopsis thaliana*. *Plant Mol. Biol.* **62**, 29–42.

Palma, K., Thorgrimsen, S., Malinovsky, F.G., Fiil, B.K., Nielsen, H.B., Brodersen, P., Hofius, D., Petersen, M. and Mundy, J. (2010) Autoimmunity in Arabidopsis *acd11* is mediated by epigenetic regulation of an immune receptor. *PLoS Pathog.* **6**, e1001137.

Perfect, S.E., Hughes, H.B., O'Connell, R.J. and Green, J.R. (1999) *Colletotrichum:* a model genus for studies on pathology and fungal-plant interactions. *Fungal Genet. Biol.* **27**, 186–198.

Rosado, C.J., Buckle, A.M., Law, R.H. *et al.* (2007) A common fold mediates vertebrate defence and bacterial attack. *Science*, **317**, 1548–1551.

Rosado, C.J., Kondos, S., Bull, T.E. *et al.* (2008) The MACPF/CDC family of pore-forming toxins. *Cell. Microbiol.* **10**, 1765–1774.

Schulze-Lefert, P. and Panstruga, R. (2011) A molecular evolutionary concept connecting nonhost resistance, pathogen host range, and pathogen speciation. *Trends Plant Sci.* **16**, 117–125.

Schwessinger, B. and Ronald, P.C. (2012) Plant innate immunity: perception of conserved microbial signatures. *Annu. Rev. Plant Biol.* **63**, 451–482.

Shimada, C., Lipka, V., O'Connell, R., Okuno, T., Schulze-Lefert, P. and Takano, Y. (2006) Nonhost resistance in *Arabidopsis-Colletotrichum* interactions acts at the cell periphery and requires actin filament function. *Mol. Plant-Microbe Interact.* **19**, 270–279.

Shirasu, K. (2009) The HSP90-SGT1 chaperone complex for NLR immune sensors. *Annu. Rev. Plant Biol.* **60**, 139–164.

Stein, M., Dittgen, J., Sánchez-Rodríguez, C., Hou, B., Molina, A., Schulze-Lefert, P., Lipka, V. and Somerville, S. (2006) *Arabidopsis* PEN3/PDR8, an ATP binding cassette transporter, contributes to nonhost resistance to inappropriate pathogens that enter by direct penetration. *Plant Cell*, **18**, 731–746.

Thordal-Christensen, H., Zhang, Z., Wei, Y. and Collinge, D.B. (1997) Subcellular localization of H_2O_2 in plants. H_2O_2 accumulation in papillae and hypersensitive response during the barley—powdery mildew interaction. *Plant J.* **11**, 1187–1194.

Torres, M.A., Dangl, J.L. and Jones, J.D. (2002) *Arabidopsis* gp91phox homologues AtrbohD and AtrbohF are required for accumulation of reactive oxygen intermediates in the plant defence response. *Proc. Natl Acad. Sci. USA*, **99**, 517–522.

Tsuda, K. and Katagiri, F. (2010) Comparing signaling mechanisms engaged in pattern-triggered and effector-triggered immunity. *Curr. Opin. Plant Biol.* **13**, 459–465.

Tsuda, K., Sato, M., Glazebrook, J., Cohen, J.D. and Katagiri, F. (2008) Interplay between MAMP-triggered and SA-mediated defence responses. *Plant J.* **53**, 763–775.

Tsuda, K., Mine, A., Bethke, G., Igarashi, D., Botanga, C.J., Tsuda, Y., Glazebrook, J., Sato, M. and Katagiri, F. (2013) Dual regulation of gene expression mediated by extended MAPK activation and salicylic acid contributes to robust innate immunity in *Arabidopsis thaliana*. *PLoS Genet.* **9**, e1004015.

Wan, J., Zhang, X.C., Neece, D., Ramonell, K.M., Clough, S., Kim, S., Stacey, M.G. and Stacey, G. (2008) A LysM receptor-like kinase plays a critical role in chitin signaling and fungal resistance in Arabidopsis. *Plant Cell*, **20**, 471–481.

Wildermuth, M.C., Dewdney, J., Wu, G. and Ausubel, F.M. (2001) Isochorismate synthase is required to synthesize salicylic acid for plant defence. *Nature*, **414**, 562–565.

Zhang, Z., Wu, Y., Gao, M., Zhang, J., Kong, Q., Liu, Y., Ba, H., Zhou, J. and Zhang, Y. (2012) Disruption of PAMP-induced MAP kinase cascade by a *Pseudomonas syringae* effector activates plant immunity mediated by the NB-LRR protein SUMM2. *Cell Host Microbe*, **11**, 253–263.

Zhao, T., Rui, L., Li, J., Nishimura, M.T., Vogel, J.P., Liu, N., Liu, S., Zhao, Y., Dangl, J.L. and Tang, D. (2015) A truncated NLR protein, TIR-NBS2, is required for activated defense responses in the *exo70B1* mutant. *PLoS Genet.* **11**, e1004945.

Zhou, N., Tootle, T.L. and Glazebrook, J. (1999) *Arabidopsis PAD3,* a gene required for camalexin biosynthesis, encodes a putative cytochrome P450 monooxygenase. *Plant Cell*, **11**, 2419–2428.

